Investigation of density and form factor of some F isotopes using Hartree-Fock and shell model calculations

Wasan Z. Majeed

Department of Physics, College of Science, University of Baghdad

E-mail: wasan_zmz@yahoo.com

Abstract

Structure of unstable ^{21,23,25,26}F nuclei have been investigated using Hartree – Fock (HF) and shell model calculations. The ground state proton, neutron and matter density distributions, root mean square (rms) radii and neutron skin thickness of these isotopes are studied. Shell model calculations are performed using SDBA interaction. In HF method the selected effective nuclear interactions, namely the Skyrme parameterizations SLy4, Skeσ, SkBsk9 and Skxs25 are used. Also, the elastic electron scattering form factors of these isotopes are studied. The calculated form factors in HF calculations show many diffraction minima in contrary to shell model, which predicts less diffraction minima. The long tail behaviour in nuclear density is noticeable seen in HF more than shell model calculations. The deviation occurs between shell model and HF results are attributed to the sensitivity of charge form factors to the change of the tail part of the charge density. Calculations done for the rms radii in shell model showed excellent agreement with experimental values, while HF results showed an overestimation in the calculated rms radii for ^{21,23}F and good agreement for ^{25,26}F. In general, it is found that the shell model and HF results have the same behaviour when the mass number (A) increase.

Key words

Shell model, Hartree – Fock, electron scattering, rms charge, neutron, and matter radii.

Article info.

Received: Apr. 2016
Accepted: May. 2016
Published: Sep. 2016

تفحص الكثافة وعامل التشكل لبعض نظائر الفلور باستخدام حسابات الهارتري- فوك ونموذج القشرة

وسن زهير مجيد

قسم الفيزياء، كلية العلوم، جامعة بغداد

الخلاصة

تركيب النوى غير المستقرة لنظائر ^{21,23,25,26}F تم تفحصه باستخدام حسابات الهارتري- فوك و نموذج القشرة. تم دراسة توزيعات كثافة الشحنة، النيوترون والمادة النووية ، انصاف الاقطار للبروتونات والنيوترونات و سمك القشرة النيوترونية لتلك النظائر. حسابات نموذج القشرة انجزت باستخدام التفاعل SDBA. في حسابات الهارتري فوك تم اختيار تفاعلات بحدود سكيرم مختلفة SLy4, Skeσ, SkBsk9 and Skxs25 . كذلك تم حساب عوامل التشكل المرنة لهذه النظائر. حسابات عوامل التشكل باستخدام الهارتري فوك اظهرت وجود نهايات صغرى اكثر من تلك المحسوبة باستخدام نموذج القشرة. الامتداد الطويل للكثافة النووية ظهر في حسابات الهارتري فوك بصورة واضحة اكثر من حسابات نموذج القشرة. لذلك ظهر الاختلاف بين نتائج نموذج القشرة والهارتري فوك بسبب اعتماد عوامل التشكل على الامتداد الموجود في كثافة الشحنة. حسابات انصاف الاقطار التي جرت باستخدام نموذج القشرة اظهرت توافق مع القيم العملية بينما حسابات الهارتري – فوك اظهرت قيم اعلى من القيم العملية للنظائر ^{21,23}F وقيم مطابقة للنظائر ^{25,26}F. بصورة عامة وجد ان نتائج نموذج القشرة تتقارب مع الهارتري فوك كلما زاد العدد الكتلي.

Introduction

Most of our knowledge of nuclear physics is obtained from the study of stable nuclei on and near the stability line [1]. The development of radioactive isotope (RI) beam techniques [2-4] has opened a new field for the study of unstable nuclei far from the stability line.

Nuclear charge density distributions are very important to understanding the internal structure of nuclei [5]. For many years, electron- nucleus scattering has proven to be an excellent tool for the study of nuclear charge size and charge distribution. In the near future, elastic electron scattering off exotic nuclei will be realized. Thus, it is interesting and necessary to study electron scattering off exotic nuclei theoretically to provide the future experiments with some useful instructions in advance [6]. Several theoretical and experimental groups have devoted their work on studying the exotic nuclei [7-12].

Chu yan-Yun et al. [13] studied the electron scattering of unstable ^{17}F, ^{18}Ne, and some neutron rich N=8 isotones nuclei using relativistic mean field theory and phase shift analysis. The ground state charge density distributions, form factors and rms radii of ^{12}C and ^{16}O nuclei were calculated in shell model by Radhi et al. [14] using core plus valence and ab- intio. Calculations are compared with the results of self-consistent mean field using selected Skyrme forces. Recently, Radhi et al. [15] studied inelastic electron scattering form factors, energy levels and transition probabilities for positive and negative low-lying states using shell model and HF calculations.

The aim of the present work is to study the nuclear density and elastic electron scattering form factors for ^{21,23,25,26}F nuclei using shell model and HF calculations. The nuclear shell model calculation is performed using *sd*- model space which consist the active shells $1d_{5/2}$, $2s_{1/2}$ and $1d_{3/2}$ above the inert ^{16}O nucleus core. USD-type Hamiltonians called SDBA [16] has been used to provided realistic *sd*-shell wave functions for ground state. The radial wave functions for the single- particle matrix elements were calculated by using the harmonic-oscillator potential (HO) and the OBDM elements are computed from the shell model code oxbash [17]. For HF method, the effective nucleon-nucleon interaction Skyrme forces SLy4 [18], Skeσ [19], SkBsk9 [20] and Skxs25 [21] parameterizations are used.

Theoretical formulations

The expectation value of the HF Hamiltonian of the system is given by [22]:

$$\langle \phi_{HF} | \hat{H} | \phi_{HF} \rangle = \sum_{i=1}^{A} \langle \phi_i | \hat{T} | \phi_i \rangle + \frac{1}{2} \sum_{ij}^{A} \langle \phi_i \phi_j | \vec{\upsilon}(i,j) | \phi_i \phi_j \rangle \quad (1)$$

where $\vec{\upsilon}(i,j)$ contains all parts of nucleon– nucleon forces. This forces consists of some two-body terms together with a three-body term [23]:

$$\hat{V}_{Skyrme} = \sum_{I\langle J} V_{ij}^{(2)} + \sum_{i\langle j \langle k} V_{ijk}^{(3)} \quad (2)$$

with

$$V_{ij}^{(2)} = t_0(1+x_0 p_\sigma)\delta(\vec{r}) + \frac{1}{2} t_1 [\delta(\vec{r})\vec{k}^2 + \vec{k}^{\sim 2}\delta(\vec{r})] + t_2 \vec{k}^{\sim} \delta(\vec{r}) \vec{k} + i W_0 (\vec{\sigma}_i - \vec{\sigma}_j) \vec{k} \times \delta(\vec{r}) \vec{k} \quad (3)$$

$$V_{ijk}^{(3)} = t_3 \delta(\vec{r}_i - \vec{r}_j) \delta(\vec{r}_j - \vec{r}_k) \quad (4)$$

the relative momentum operators $\vec{k} = (\nabla_i - \nabla_j)/2i$, acting to the right and $\vec{k}^{\sim 2} = -(\nabla_i - \nabla_j)/2i$, acting to the left.

In the shell model calculations, the ground state density distribution takes the form

$$\rho_{t_z}(r)=\frac{1}{4\pi\sqrt{(2J_i+1)}}\sum_{a}\sqrt{2j_a+1}X^{J_i,J_i,0}_{a,a,t_z}\left|R_{n_a l_a}(r,b_{t_z})\right|^2 \qquad (5)$$

$R_{n\,l}(r)$ is the radial part of the HO wave function and $X^{J_f,J_i,J}_{a,a,t_z}$ is the proton $(t_z = 1/2)$ or neutron $(t_z = -1/2)$ one body density matrix element.

The matter density distribution of Eq.(5) may also be expressed as

$$\rho_m(r) = \rho_p(r) + \rho_n(r) \qquad (6)$$

The corresponding rms radii are given by

$$\left\langle r^2 \right\rangle_g^{1/2} = \frac{4\pi}{g}\int_0^\infty dr\ r^4 \rho_g(r) \qquad (7)$$

where g represents the corresponding number of nucleons.

The neutron skin thickness (t), can be defined as

$$t = r_n - r_p \qquad (8)$$

The corresponding elastic scattering (J=0) form factor (C0) is written in the following form

$$F_{0.t_z}(q)=\frac{4\pi}{g}\int_0^\infty dr r^2 \rho_g(r) j_0(qr)\ F_{fs}(q)F_{cm}(q) \qquad (9)$$

where $F_{fc}(q)$ and $F_{cm}(q)$ are free nucleon form factor and center of mass correction, respectively, given by [24]:

$$F_{fs}(q) = [1+(q/4.33\ fm^{-1})^2]^{-2} \qquad (10)$$

and

$$F_{cm}(q) = e^{q^2b^2/4A} \qquad (11)$$

where A in Eq. (9) represents the mass number of the nucleus under study.

Results and discussion

In order to explain the nuclear structure of unstable ^{21,23,25,26}F nuclei nuclear radii, nuclear density distributions and form factors are studied using shell model calculations with *sd*- model space which consist the active shells $1d_{5/2}$, $2s_{1/2}$ and $1d_{3/2}$ above the inert ^{16}O nucleus core. USD-type Hamiltonians called SDBA [16] has been used to provided realistic *sd*-shell wave functions for ground state. Also, self-consistent mean field with selected Skyrem forces (SLy4, Skeσ, SkBsk9 and Skxs25) are used. The HO size parameters for ^{21}F, ^{23}F, ^{25}F and ^{26}F are taken to be (1.77, 1.71, 1.9 and 2) fm, respectively.

The calculated proton, neutron and matter rms radii with neutron skin thickness (t) are tabulated and compared with experiment data in Tables 1 to 4 for ^{21}F, ^{23}F, ^{25}F and ^{26}F, respectively. From these tables, it clear that the calculated rms using shell model calculation gives excellent agreement with available experimental data. The results of HF showed an overestimation in the calculated rms radii for ^{21}F and ^{23}F, while these results are quite consistent with the experimental values for ^{25}F and ^{26}F. From the results one can see that the shell model and HF calculations coincide with each other with increasing of mass number (A). Also, the calculated rms of proton, neutron, matter and neutron skin thickness with shell model and the Skyrme HF have approximately been increased with increasing of number of neutron.

Table 1: The values of rms radii in fm of ^{21}F nucleus.

Model	$\langle r\rangle_p^{1/2}$ fm	$\langle r\rangle_n^{1/2}$ fm	t fm	$\langle r\rangle_m^{1/2}$ fm	Exp. $\langle r\rangle_m^{1/2}$ fm [25]
Sly4	2.802	2.961	0.159	2.894	2.71±0.03
Skeσ	2.744	2.861	0.117	2.811	
SkBsk9	2.77	2.934	0.164	2.867	
Skxs25	2.807	2.994	0.187	2.916	
Shell model	2.628	2.777	0.149	2.714	

Table 2: The values of rms radii in fm of ^{23}F nucleus.

Model	$\langle r\rangle_p^{1/2}$ fm	$\langle r\rangle_n^{1/2}$ fm	t fm	$\langle r\rangle_m^{1/2}$ fm	Exp. $\langle r\rangle_m^{1/2}$ fm [25]
Sly4	2.803	3.038	0.235	2.948	2.79±0.04
Skeσ	2.753	2.922	0.169	2.857	
SkBsk9	2.781	3.024	0.243	2.931	
Skxs25	2.8	3.098	0.298	2.985	
Shell model	2.64	2.88	0.24	2.773	

Table 3: The values of rms radii in fm of ^{25}F nucleus.

Model	$\langle r\rangle_p^{1/2}$ fm	$\langle r\rangle_n^{1/2}$ fm	t fm	$\langle r\rangle_m^{1/2}$ fm	Exp. $\langle r\rangle_m^{1/2}$ fm [25]
Sly4	2.834	3.214	0.380	3.08	3.12±0.08
Skeσ	2.798	2.97	0.172	2.909	
SkBsk9	2.813	3.198	0.385	3.065	
Skxs25	2.816	3.272	0.456	3.115	
Shell model	2.936	3.221	0.285	3.121	

Table 4: The values of rms radii in fm of ^{26}F nucleus.

Model	$\langle r\rangle_p^{1/2}$ fm	$\langle r\rangle_n^{1/2}$ fm	t fm	$\langle r\rangle_m^{1/2}$ fm	Exp. $\langle r\rangle_m^{1/2}$ fm [25]
Sly4	2.855	3.305	0.45	3.156	3.23±0.13
Skeσ	2.817	3.128	0.311	3.024	
SkBsk9	2.836	3.285	0.449	3.137	
Skxs25	2.840	3.360	0.52	3.190	
Shell model	3.091	3.412	0.321	3.305	

Figs. 1, 2, 3 and 4 display the calculated proton density distributions obtained with shell model (black curve) and HF using SLy4, Skeσ, SkBsk9 and Skxs25 as red, blue, green and violet curves, respectively. It is evident from these figures that the calculated proton densities are all have the same behavior for the Skrme forces and shell model in the central region. The obtained values of the proton density for these isotopes at center region and the long tail (which is noticeably seen in the distribution of the density at r > 4 fm) decreased with increasing number of neutron.

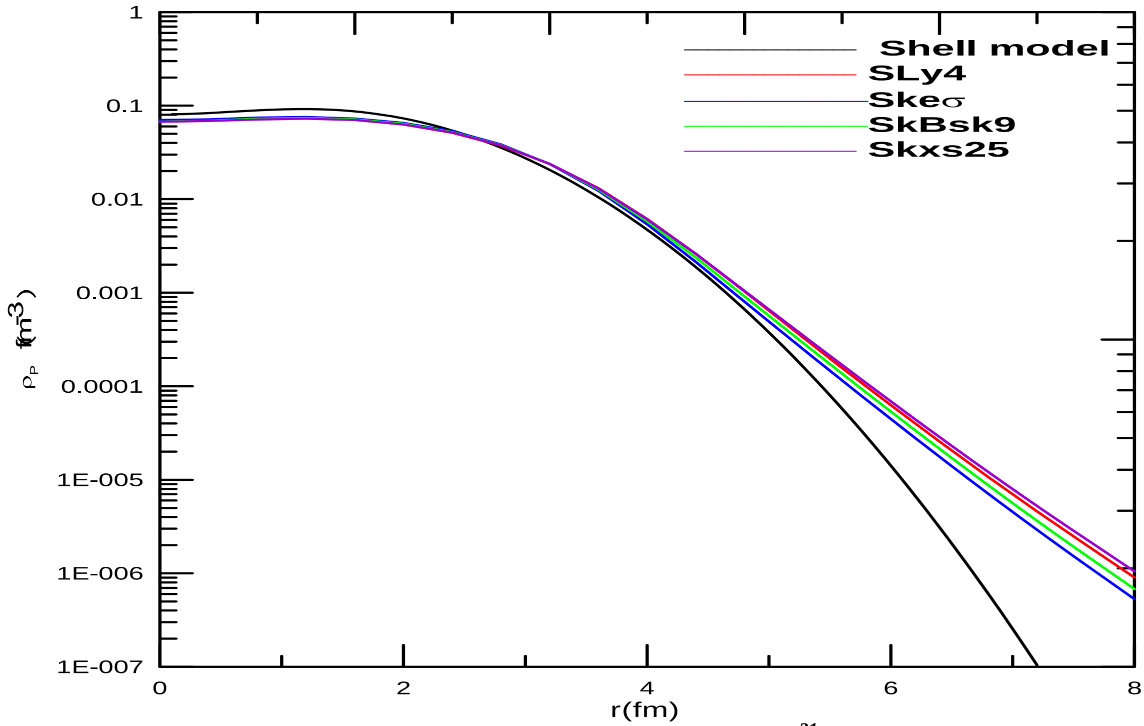

Fig.1: Proton density distributions of ^{21}***F.***

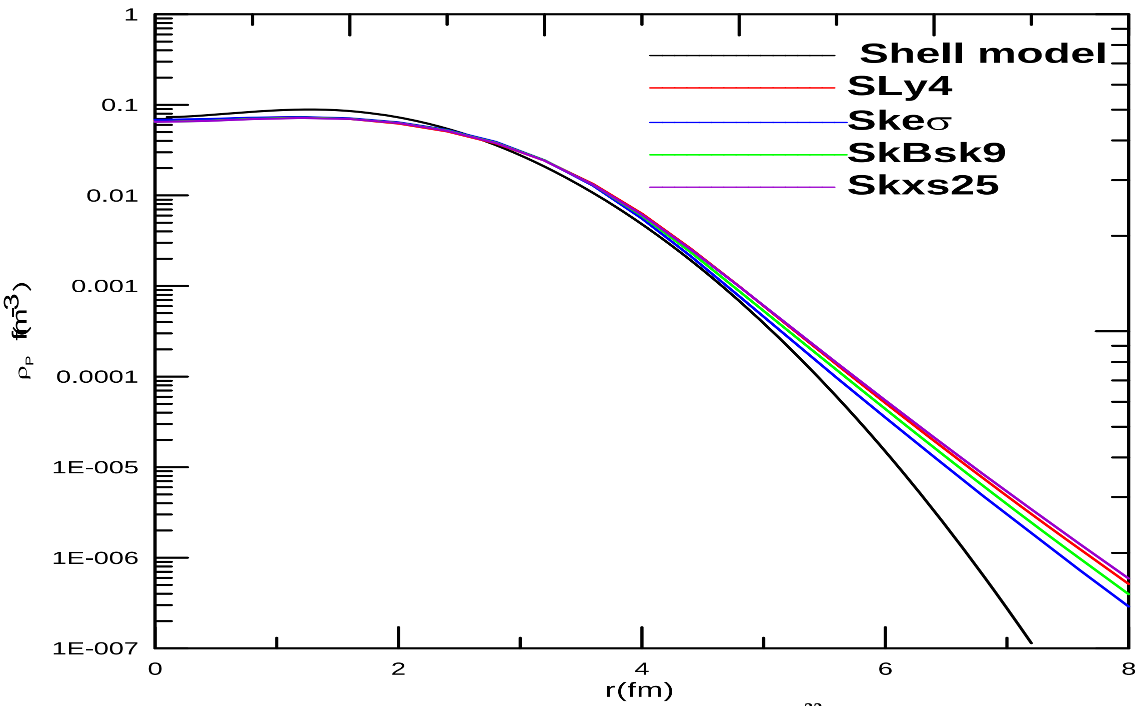

Fig.2: Proton density distributions of ^{23}***F.***

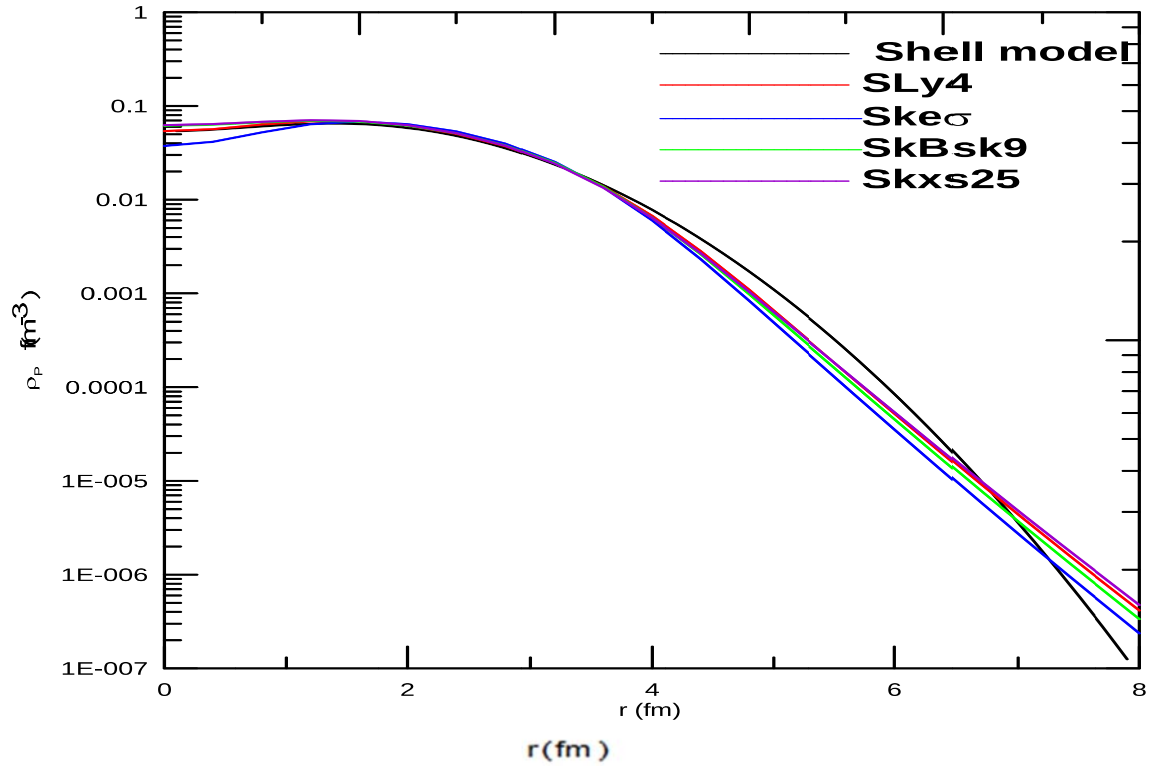

Fig.3: Proton density distributions of ^{25}F.

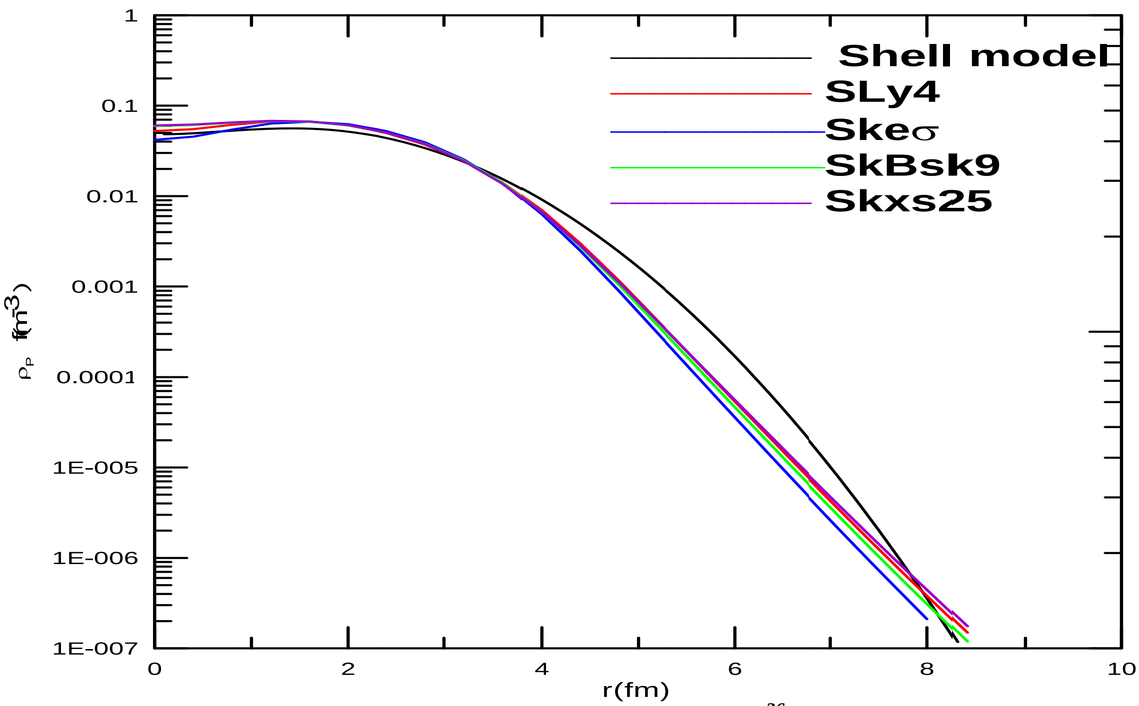

Fig.4: Proton density distributions of ^{26}F.

The neutron density distributions of these isotopes are displayed in Figs. 5, 6, 7 and 8. These figures showed that the results of HF calculations have the same behavior through the whole range of r and differ from the shell model results at fall-off region. The long tail behaviour is noticeable seen in HF more than shell model calculation. The obtained values of the neutron density for these isotopes at center region increased with increasing of the number of neutron. The matter density distribution of these nuclei are displayed in Figs. 9, 10, 11 and 12. For comparison the available experimental data of matter density distributions for ^{26}F denoted as shaded area [25] are displayed in Fig. 12. It is clear from this figure that the calculated density with HF and shell model calculations give good agreement with the experimental data indicated with its error bars by the shaded area.

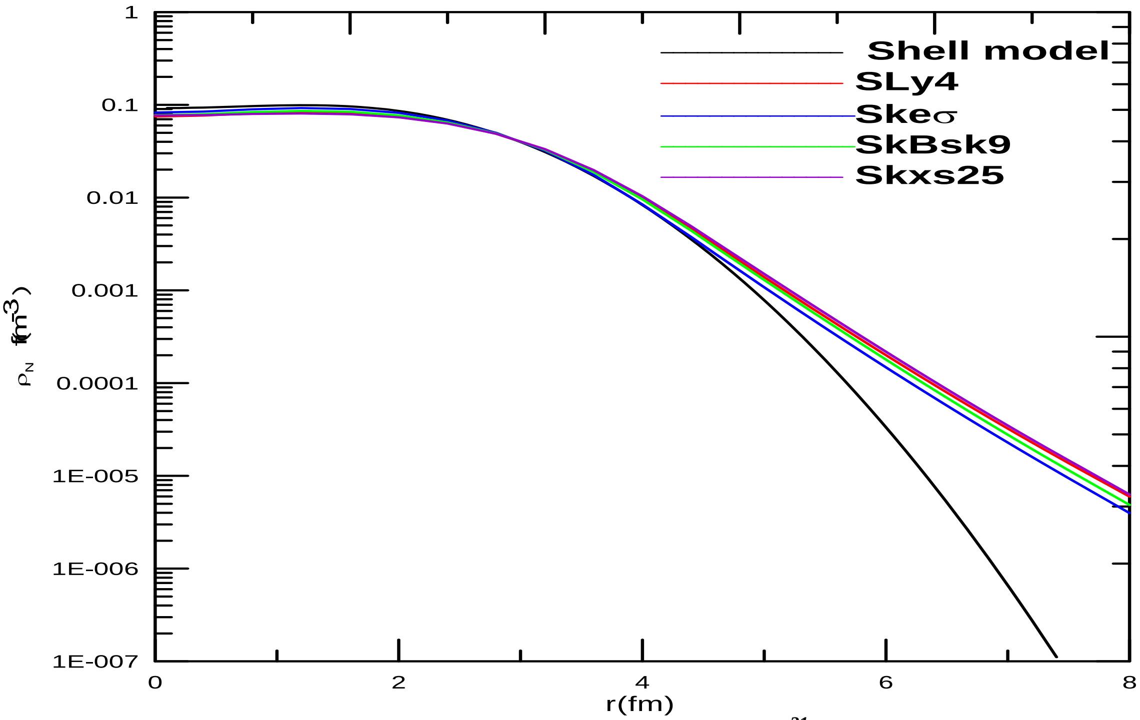

Fig.5: Neutron density distributions of ^{21}F.

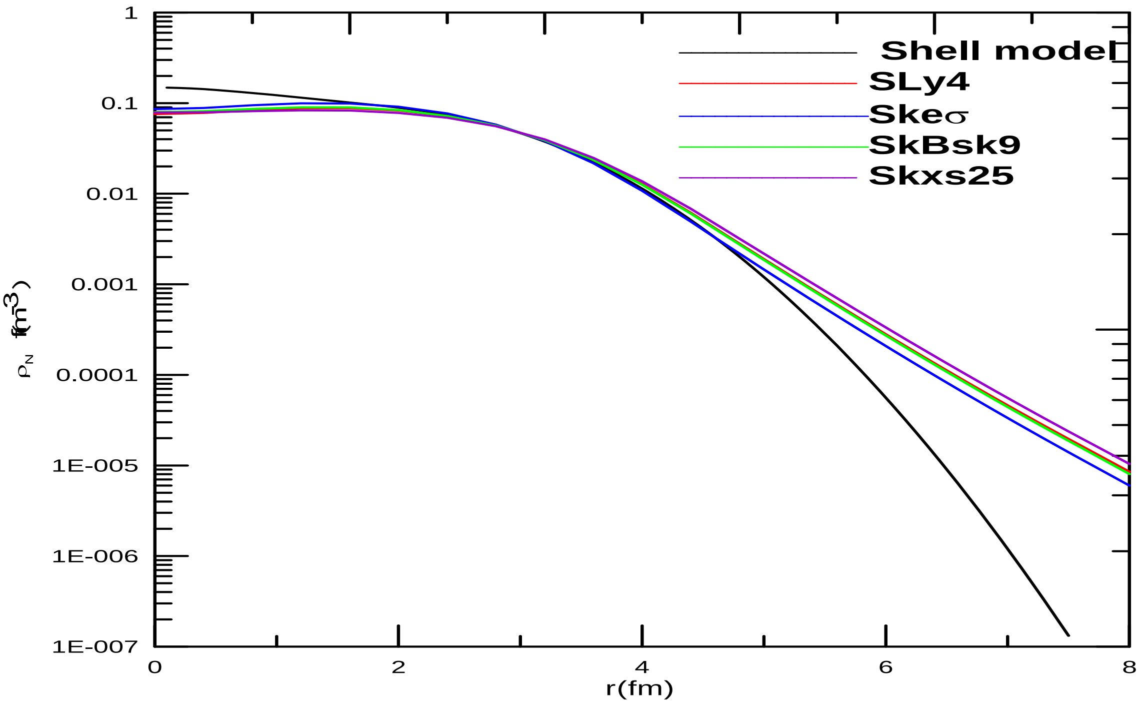

Fig.6: Neutron density distributions of ^{23}F.

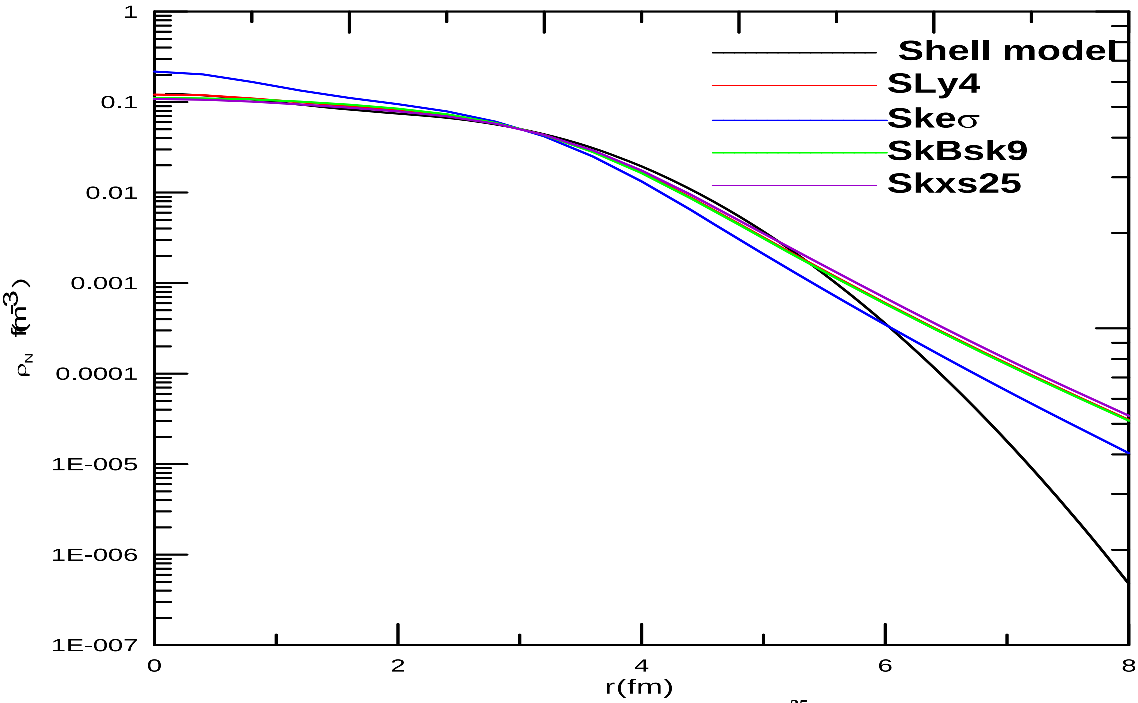

Fig.7: Neutron density distributions of ^{25}F.

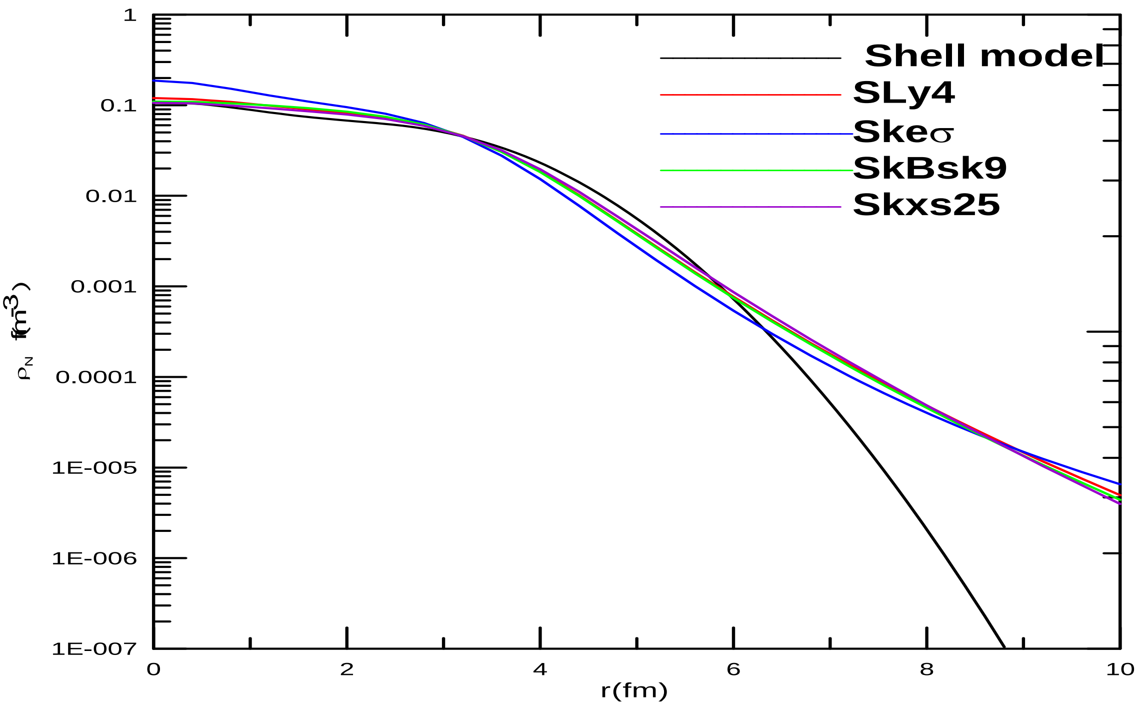

Fig.8: Neutron density distributions of ^{26}F.

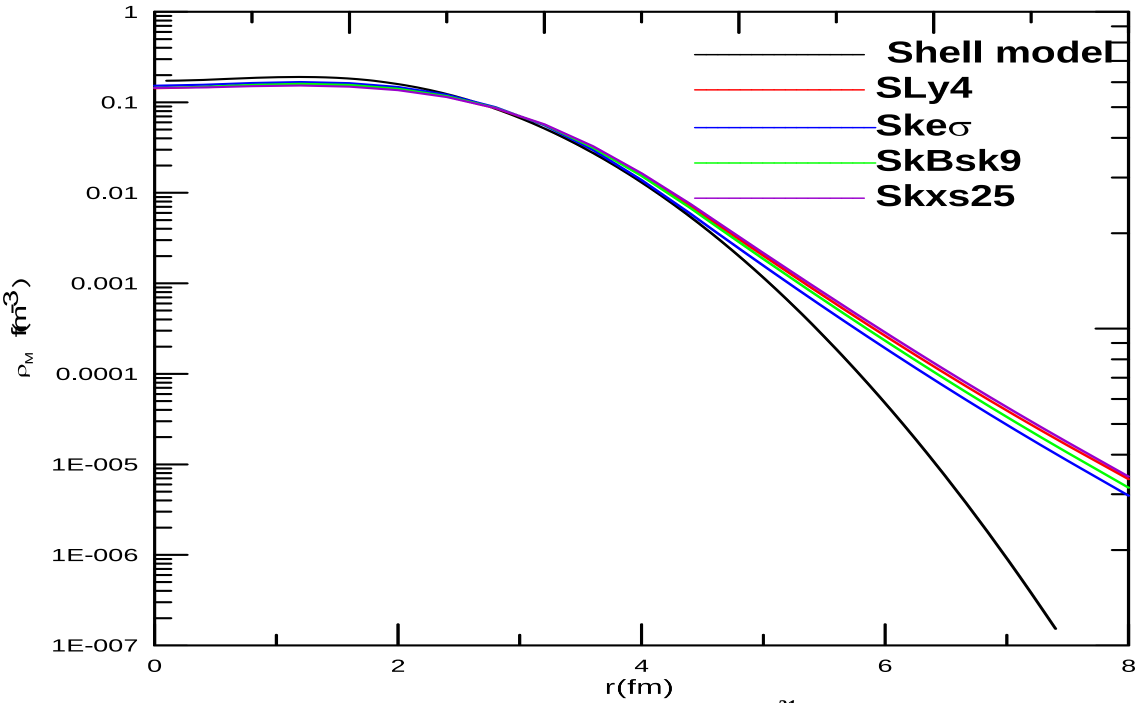

Fig.9: matter density distributions of ^{21}F.

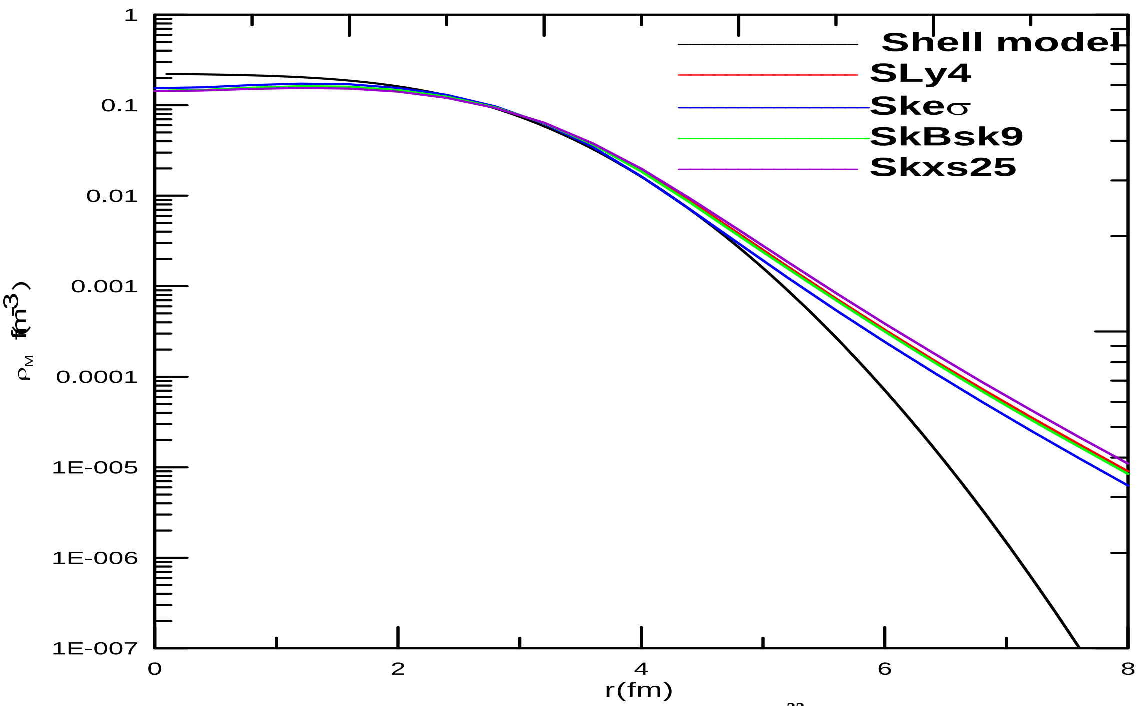

Fig.10: matter density distributions of ^{23}F.

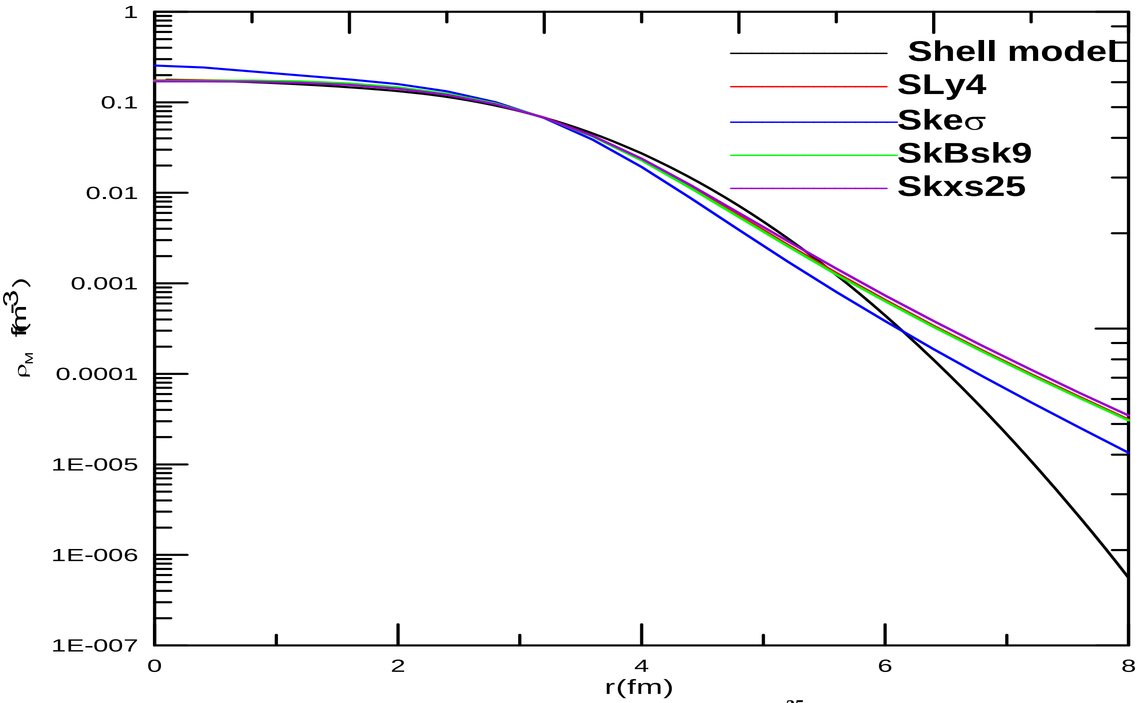

Fig.11: matter density distributions of ^{25}F.

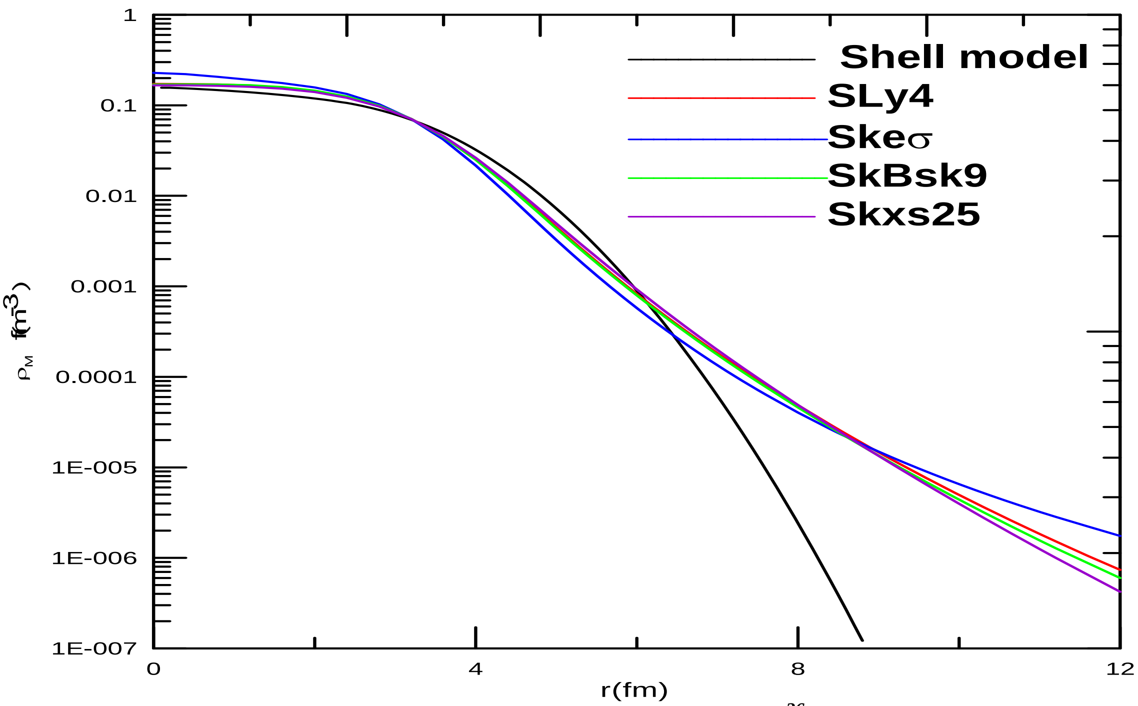

Fig.12: matter density distributions of ^{26}F.

In Figs.13, 14, 15 and 16, the calculated elastic form factors are plotted. The black, red, blue, green and violet curves represent the shell model and HF with SLy4, Skeσ, SkBsk9 and Skxs25 calculations. For the sake of completeness of comparison, ^{19}F is chosen as a reference of the stable nucleus, where experimental data of electron scattering form factors are available [26]. These figures give the conclusion that the form factors is not dependent on detailed properties of the distributions of neutron density.

It is apparent from Fig. 13 that the HF calculations for all Skyrme almost coincide in range of q < 1.5 fm^{-1}. The deviation occurs between shell model and HF results at q >1 fm^{-1}, since the form factors are sensitive to the change in the tail part of the charge density. As one can see that both of shell model and experimental data has one diffraction minimum. The location of the minimum of shell results has forward shift as compared with the minimum of HF results. The longitudinal C0 elastic electron scattering form factors of ^{23}F nucleus are shown in Fig. 14. These form factors are connected with the proton density distribution. It is found from this figure that all HF results has two diffraction minimum, while shell model results has only one. The location of the minimum of shell results has forward shift as compared with the minimum of HF results. Figs.15 and 16 show the calculated electron scattering form factors of ^{25}F and ^{26}F respectively. In these figures, all results predicted approximately the same position of the diffraction minimum. Also, the results of Skeσ differ from other results of HF calculation and becomes upward at high momentum transfers.

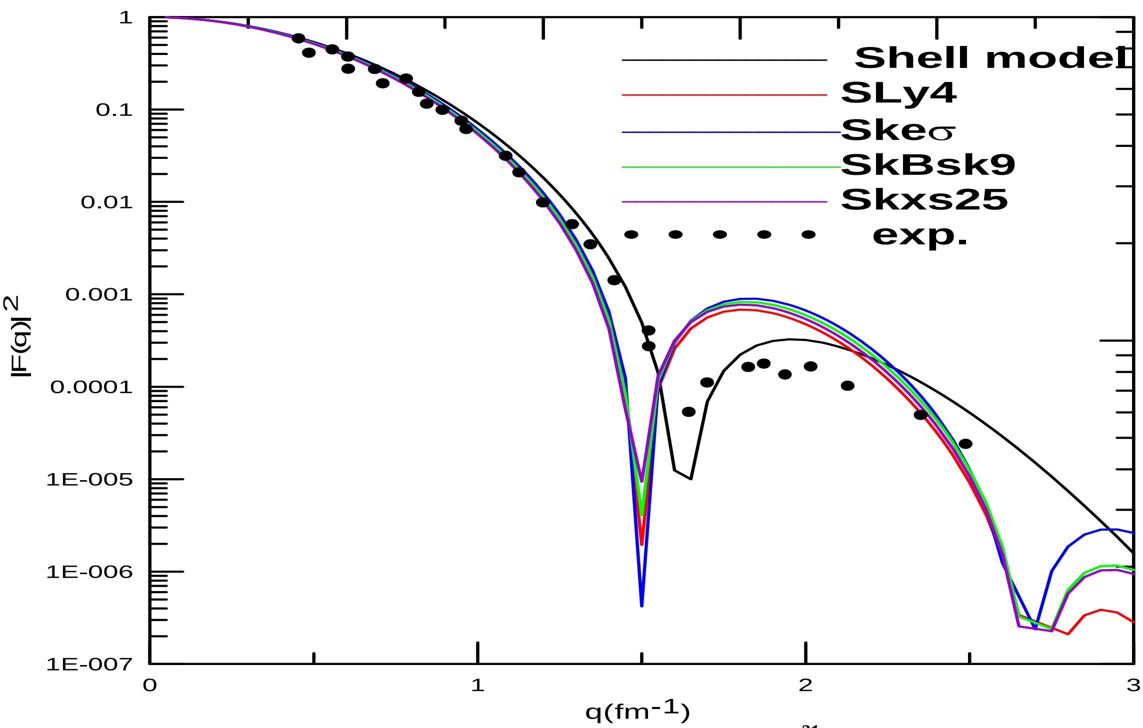

Fig.13: Elastic charge form factors of ^{21}F.

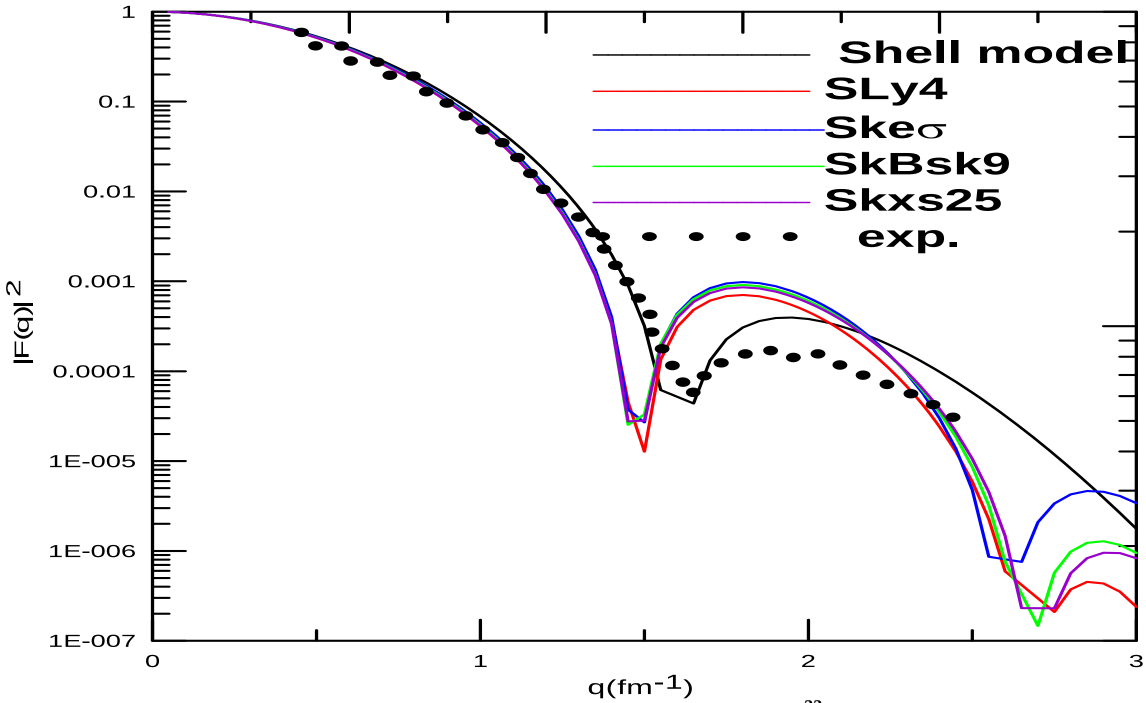

Fig.14: Elastic charge form factors of ^{23}F.

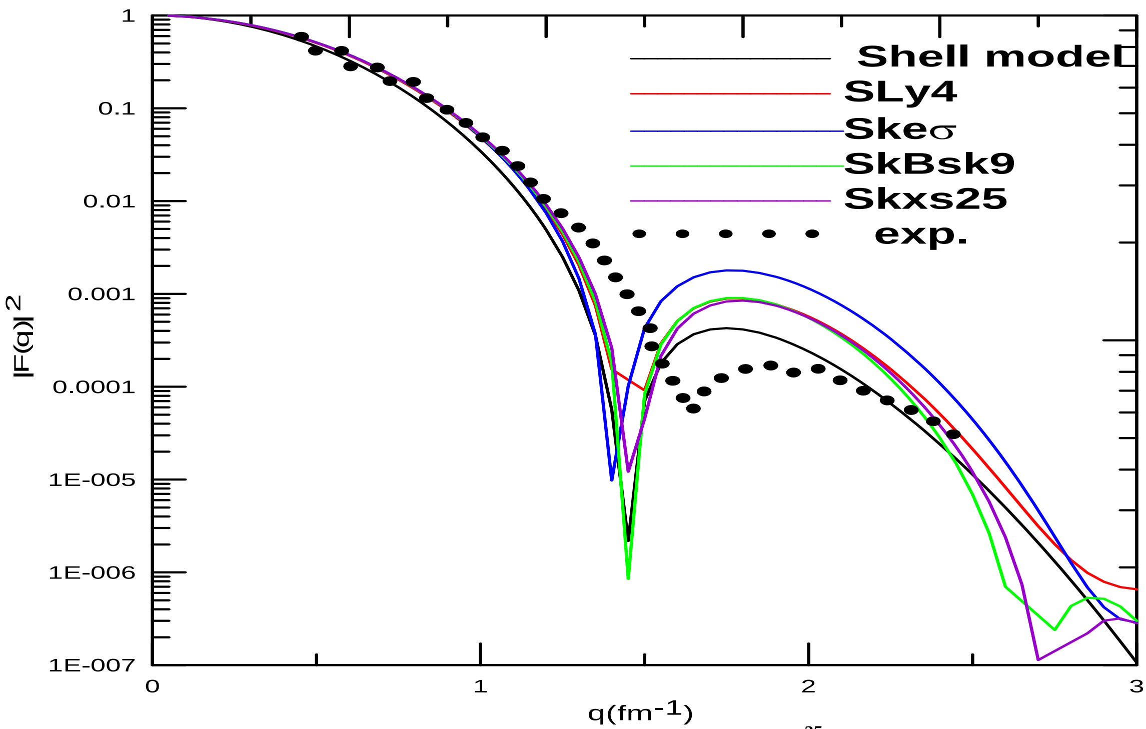

Fig.15: Elastic charge form factors of ^{25}F.

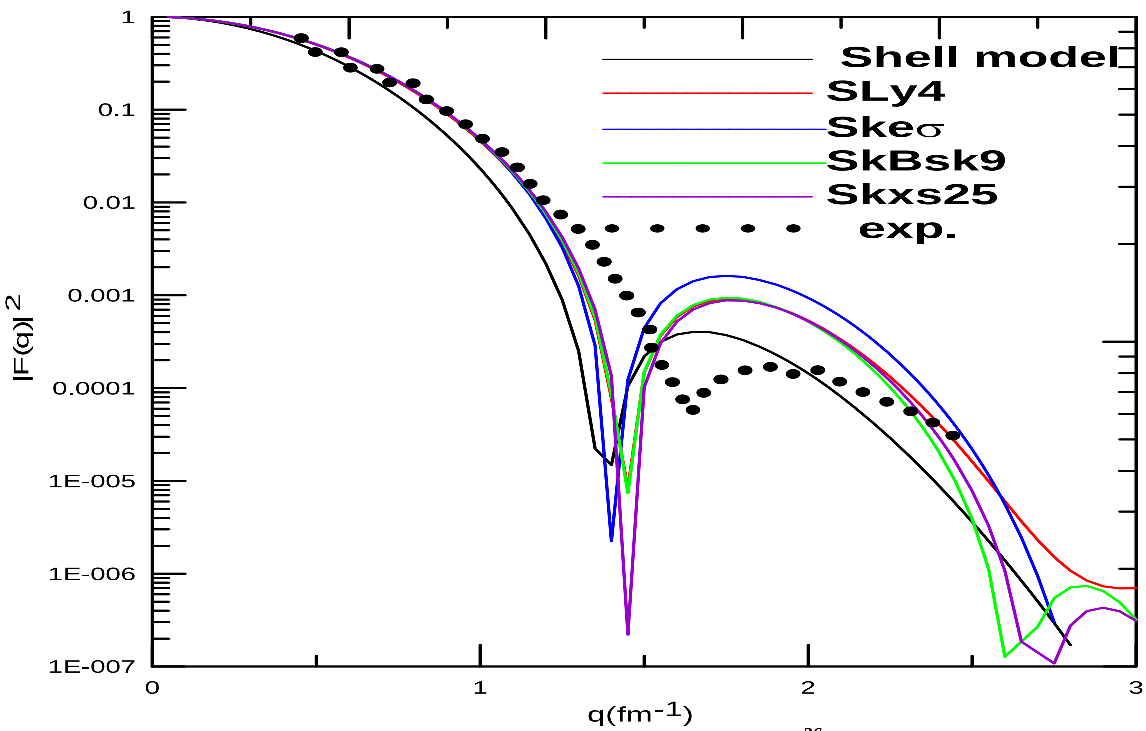

Fig.16: Elastic charge form factors of ^{26}F.

Conclusion

In this study, structure of unstable ^{21,23,25,26}F isotopes have been investigated using shell model and HF calculations. In shell model calculations, results of rms radii showed excellent agreement with experimental data, while HF results showed an overestimation in the calculated rms radii for ^{21,23}F and good agreement for ^{25,26}F. In general, it is found that the shell model and Hartree – Fock results all have the same behaviour when the mass number (A) increase. The calculated rms of proton, neutron, matter and neutron skin thickness with shell model and the Skyrme HF have approximately been increased with increasing number of neutron. It is clear from the result of the density distribution that the calculated density are quite consistent with all the Skrme forces and shell model in the central region. It is useful to remark that the obtained values of the proton density for these isotopes at this region decreased with increasing number of neutron, while the neutron density has increased. The long tail behaviour in neutron density is noticeable seen in HF more than shell model calculation. Thus, in form factors calculations the deviation occurs between shell model and HF results since the form factors are sensitive to the change of the tail part of the charge density. As one can see that each HF results has two diffraction minimum, while shell model results has only one

References

[1] Z. Wang, Z. Ren, Y. Fan, Phys. Rev. C73 (2006) 014610.

[2] I. Tanihata, Prog. Part. Nucl. Phys. 35 (1995) 505.

[3] H. Geissel, G. Munzenberg, K. Riisager, Ann. Rev. Nucl. Part. Sci. 45 (1995) 163.

[4] A. C. Mueller, Prog. Part. Nucl. Phys. 46 (2001) 359.

[5] Z. Wang and Z. Ren, Phys. Rev. C71 (2005) 054323.

[6] Y. Chu, Z. Ren, T. Done, Z. Wang, Phys. Rev. C79 (2009) 044313.

[7] S. R. Neumaier, G. D. Alkhazov, M. N. Andronenko, A. V. Dobrovolsky, P. Egelhof, G. E.

Gavrilov, H. Geissel, H. Irnich, A. V. Khanzadeev, G. A. Korolev, A. A. Lobodenko, G. Munzenberg, M. Mutterer, W. Schwab, D. M. Seliverstov, T. Suzuki, N. A. Timofeev, A. A. Vorobyov, V. I. Yatsoura, Nucl. Phys. A 712 (2002) 247.
[8] A. V. Dobrovolsky, G. D. Alkhazov, M. N. Andronenko, A. Bauchet, P. Egelhof, S. Fritz, H. Geissel, C. Gross, A. V. Khanzadeev, G. A. Korolev, G. Kraus, A. A. Lobodenko, G. Munzenberg, M. Mutterer, S. R. Neumaier, T. Schafer, C. Scheidenberger, D. M. Seliverstov, N. A. Timofeev, A. A. Vorobyov, V. I. Yatsoura, Nucl. Phys. A 766 (2006) 1.
[9] H. Z. Guo, W. Meng, X. H. Shan, S. Z. Yu, W. J. Song, X. G. Qing, Z. W. Long, X. Z. Gang, M. R. Shi, L. Chen, Z. X. Ying, Z. H. Bin, Z. T. Cheng, X. Z. Guo, W. Yue, C. R. Fu, H. T. Heng, F. Fen, G. Qi, H. J. Long Z. X. Heng, Z. Chuan, Y. Y. Hong, G. Z. Yan Science in China, G51 (2008) 781.
[10] L. J. Xing, L. P. Ping, W. J. Song, H. Z. Guo, M. R. Shi, S. Z. Yu, L. Chen, C. R. Fu, X. H. Shan, X. G. Qing, X. G. Qing, G. Z. Yan, Chinese Phys. C 34 (2010) 452.
[11] H. T. Fortune and R. Sherr, Eur. Phys. J. A47 (2011) 154.
[12] R. A. Radhi, A. K. Hamoudi, A. Rifat, Iraqi Journal of Science, 54 (2013) 324.
[13] Y. Chu, Z. Ren, Z. Wang, T. Dong, Commun. Theor. Phys. (Beijing, China) 54 (2010) 347.
[14] R. A. Radhi, A. Rifaah, W. Z. Majeed, Indian J. Phys. 89 (2015) 723.
[15] R. A. Radhi, A. A. Alzubadi, E. M. Rashed, Nucl. Phys. A 947 (2016) 12.
[16] M. H. Jensen, T. S. Kuo, E. Osnes, Phys. Rep. 261 (1995) 125.
[17] B. A. Brown, A. Etchegoyen, N. S. Godwin, W. D. M. Rae, W. A. Richter, W. E. Ormand, E. K. Warburton, J. S. Winfield, L. Zhao, C. H. Zimmerman, MSU-NSCL report number 1289 (2005 version).
[18] E. Chabanat, P. Bonche, P. Haensel, J. Meyer, R. Schaeffer, Nucl. Phys. A 635 (1998) 231.
[19] J. Friedrich and P. G. Reinhard, Phys. Rev. C33 (1986) 335.
[20] S. Goriely, M.Samyn, J. M. Pearson, M. Onsi, Nucl. Phys. A 750 (2005) 425.
[21] B. A. Brown, G. Shen, G. C. Hillhouse, J. Meng, A. Trzcinska, Phys. Rev. C76 (2007) 034305.
[22] L. Guo-qiang, Commun. Theor. Phys. 13 (1990) 457.
[23] D. Vautherin, D. M. Brink, Phys. Rev. C5 (1972) 626.
[24] J. P. Glickman, W. Bertozzi, T. N. Buti, S. Dixit, F. W. Hersman, C. E. Hyde- Wright, M. V. Hynes, R. W. Lourie, and B. E. Norum, J. J. Kelly, Phys. Rev. C43 (1990) 1740.
[25] A. Ozawa, T. Suzuki, I. Tanihata, Nucl. Phys. A 693 (2001) 32.
[26] T. Sakuda, Prog. Theor. Phys., 87 (1992) 1159.